Acta virologica 56: 227 – 233, 2012 doi:10.4149/av_2012_03_227

A mouse model of swine influenza virus H9N2 infection with acute lung injury

WEI DONG[1,2], XIE LI-FENG[2], WANG CUN-LIAN[2], XU MING-JU[2], ZHANG RUI-HUA[2], LIU YING[1*], XU TONG[2*]

[1]Department of Basic Veterinary Medicine, College of Veterinary Science, Gansu Agricultural University, Lanzhou, 730070, Gansu, P. R. China; [2]Department of Veterinary Medicine, College of Animal Science, HeBei North University, Zhangjiakou, 075131, Hebei, P. R. China

Received January 9, 2012; accepted August 20, 2012

Summary. – BALB/c mice inoculated intranasally with A/swine/HeBei/012/2008/ (H9N2) virus (SIV), showing acute lung injury (ALI)/acute respiratory distress syndrome (ARDS), were observed for morbidity (lung histopathology, lung coefficient, lung wet/dry weight (W/D) ratio, arterial blood gas characteristics and inflammatory cells in bronchial alveolar lavage fluid (BALF)) and mortality. The results showed that, (1) on days 1–4 post infection (p.i.), mice appeared depressed and showed ruffled fur, reduced food intake, weight loss and hypoxemia with a decreased arterial partial oxygen pressure and an increased partial carbon dioxide pressure. (2) From day 4 p.i., mice began to die and showed pulmonary edema, hemorrhage and inflammatory cells in the alveolar exudate. The lung coefficient and lung W/D ratio significantly increased. (3) On days 3–8 p.i., inflammatory cells, especially alveolar macrophages and polymorphonuclears (PMNs) in BALF significantly increased. (4) The mortality rate reached 62.5%. This study established a successful animal model of ALI induced by infection with H9N2 SIV which may help in further investigations of the pathogenesis of human ALI/ARDS induced by H9N2 SIV infection.

Keywords: swine influenza virus; H9N2 subtype; acute lung injury; mouse

Introduction

Acute lung injury (ALI) is a type of a clinical syndrome comprising of inflammation and increased permeability in the lungs that result in characteristic pathology of diffuse lung cells damage, edema and micro-atelectasis, and disorders typical for gas exchange. ALI is observed during various conditions including severe infection, trauma, shock, and toxic poisoning. It is identified by the presence of injured alveolar epithelial and endothelial cells that lead to diffuse interstitial lung disease and alveolar edema, as well as acute low oxygen respiratory insufficiency (Bernard *et al.,* 1994; Bernard, 2005). Studies indicate that the mortality rate of ALI/ARDS is 40%~60% so far (Fagan *et al.,* 1999; Hudson and Steinberg, 1999). In recent years, both severe acute respiratory syndrome and human-avian influenza viruses have caused serious lung infections and ALI, and also increase in the incidence of ARDS and high mortality. Hence, infections, especially the viral infections, have become one of the important causes of ALI/ARDS, and have drawn the attention of the scientific community worldwide.

H9N2 subtype influenza virus is one of the main virus subtypes responsible for increased morbidity and mortality in the poultry. Human infections with H9N2 virus which displayed mild respiratory disease signs were recorded in 1999 and 2003 in Hong Kong and mainland of China (Butt *et al*., 2005; Lin *et al*., 2000). Genetic analysis showed that H9N2 virus had partial genetic information similarity with

*Corresponding authors: E-mail: xutong1969@sohu.com; liny11@gsau.edu.cn; phone: +86-313-4029336.

Abbreviations: ALI = acute lung injury; ARDS = acute respiratory distress syndrome; BALF = bronchial alveolar lavage fluid; $PaCO_2$ = partial pressure of arterial carbon dioxide; PaO_2 = partial pressure of arterial oxygen; p.i. = post infection; PMNs = polymorphonuclears; SaO_2 = oxygen hemoglobin saturation; SIV = swine influenza virus; W/D ratio = wet/dry weight ratio

that of H5N1 virus which gave rise to human deaths in Hong Kong in 1997 (Lin *et al*., 2000). Further studies showed that the H9N2 virus had specific receptor which bound to human respiratory epithelial cells (i.e. Leu 226) (Wan and Perez, 2007). In addition, studies have confirmed the ability of the H9N2 virus to cross the species barrier from the poultry to mammals and its higher positive infection rate among pigs in China (Cong *et al*., 2007, 2008; Yu *et al*., 2008). Meanwhile, H9N2 subtype virus and humanized H3N2 subtype virus were found to be transmitted to pigs simultaneously (Peiris *et al.,* 2001) which provided the environment for the recombination of H9N2 subtype virus. Hence, it seems that H9N2 subtype virus circulating in pigs has potential threat to cause novel influenza pandemics in human in future. H9N2 SIV has important significance in public health and in studies on pathogenic mechanisms of H9N2 SIV in mammals. Especially, the studies on lung injury mechanisms will be of important significance for the prevention and treatment of potential human infections in the future.

Since there was so far no study on H9N2 SIV infection of mammals with pulmonary impairment, we attempted to analyze such an infection of mice and thus lay foundation for further studies on the mechanism of pulmonary impairment in mammals infected with H9N2 SIV.

Materials and Methods

Virus. A/swine/HeBei/012/2008 (H9N2) virus was inoculated into 10-day-old SPF chicken embryos (Beijing Laboratory Animal Research Center, China) and was consecutively blind passaged for 3 generations. The allantoic fluid was collected and stored at -70°C.

Experiments on mice. Eighty 6–8-week-old SPF BALB/c female mice (Beijing Laboratory Animal Research Center, China) were divided into 2 groups of 40 mice each. The mice were intranasally inoculated with H9N2 SIV (0.1 ml, containing $1\times10^3ID_{50}$) and control mice by the same dose of noninfectious allantoic fluid, which had been diluted 1:5 by sterile saline buffer. The inoculated mice were separated and kept in the bio-safety level 3+ laboratories with access to water and food ad libitum. Eight mice from the two groups were monitored daily for morbidity by measuring the weight loss, food intake, clinical signs as well as mortality. The study was approved by the Animal Care Committee of Hebei North University (Zhangjiakou, China).

Histopathology. Four mice of each group were weighed and sacrificed on days 2, 4, 6, 8, and 14 p.i. Left lobes of lungs were fixed either in 10% formalin or 4% paraformaldehyde and embedded in paraffin or Epon, respectively. The samples for microscopic examination were stained with hematoxylin and eosin. The samples for ultrastructural examination were stained with uranyl acetate and lead citrate, and were examined in a transmission electron microscope operated at 80 kV (Hitachi model H-7650, Hitachi corp., Japan).

Lung coefficient and lung W/D ratio. The mice were sacrificed as described above, and the whole wet lungs were weighed to assess lung coefficient. The W/D ratios were determined by weighing the right lung before and after oven desiccation at 80°C. W/D ratio was used as an indicator of lung edema (Majeski *et al*., 2003).

Blood gas analysis. Blood gas analysis was conducted as described by Fagan (Fagan *et al.,* 2004). Briefly, four mice of each group were anaesthetized slightly with pentobarbital sodium and arterial blood samples (0.4 ml) were collected in the heparinized syringe by percutaneous left ventricular puncture. Blood gas analysis was conducted with an IL/1620 full-automatic blood gas analyzer at once (Fagan *et al.,* 1999).

BALF inflammatory cells. Another three mice of each group were sacrificed on days 2, 4, 6, 8, and 14 p.i. BALF was collected and cell count was done as described by Xu and co-workers (Xu *et al*., 2006).

Statistical analysis. All data were expressed as means ± SD. Statistical analysis was performed with the SPSS statistical software package for Windows, version 13.0 (SPSS, Inc., USA). Differences between groups were examined for statistical significance by two-tailed Student *t* test. The *p*-values less than 0.05 were considered statistically significant.

Results

Clinical and gross pathological observations

On day 2 p.i., infected mice showed slight depression, inappetence, inactivity and ruffled fur. By the day 3 p.i., most mice presented abrupt deprementia, clinical signs of respiratory disease, including visual signs of labored respirations and respiratory distress. They also exhibited more severe inappetence, emaciation, with weight decreased to about 80% compared to that of normal mice (Fig. 1). First mice died on day 3 p.i. and overall 62.5% of mice (5 of 8) died during the experiment. Lungs of the infected mice were highly edematous, with profuse areas of hemorrhage and congestion. No obvious gross lesions were observed in other organs, including brain.

Histopathology of lungs

On day 2 p.i., lung histopathology was characterized by interstitial edema around the small blood vessels and bronchiole with inflammatory cell exudate. Neutrophil cells, erythrocytes, plenty of mucinous exudates, and edema fluid were observed in the alveolar lumen (Fig. 2b). On day 4 p.i., alveolar walls were thickened, the alveolar lumen diminished, and pulmonary interstitium broadened. In addition, obvious edema was present in interstitium around vessels and bronchiole, and parts of bronchial epithelium necrosed and sloughed. Moreover, plenty of erythrocytes appeared

in alveolar lumen and interstitium (Fig. 2c). On day 6 p.i., plenty of inflammatory cells were exuded and bronchopneumonia developed (Fig. 2d). In comparison, lungs from mock-infected mice had no apparent histopathological lesions (Fig. 2a).

Electron microscopy of lung tissues

Ultrastructural observation by transmission electron microscopy showed cell edema, cytomembrane rupture, and cytoplasm showed vacuolar degeneration. The cell nucleus edema with nucleolar margination was obvious. Edema also appeared on mitochondria where the cristae were shortened, matrix was reduced, and cytoplasm showed vacuolar degeneration (Fig.3a). The alveolar lumen also showed evidence of hemorrhage with abundant erythrocyte. Evidence of

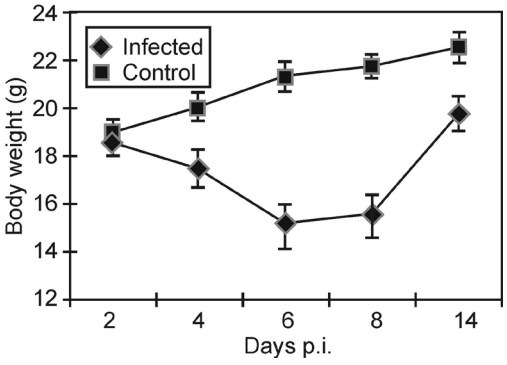

Fig.1

Effect of SIV infection on body weight of mice

Results of body weight for the eight H9N2 SIV-infected mice (♦) compared to the group of mock-infected mice with same dose of noninfectious allantoic fluid (■). The mice were monitored daily for 14 days p.i.

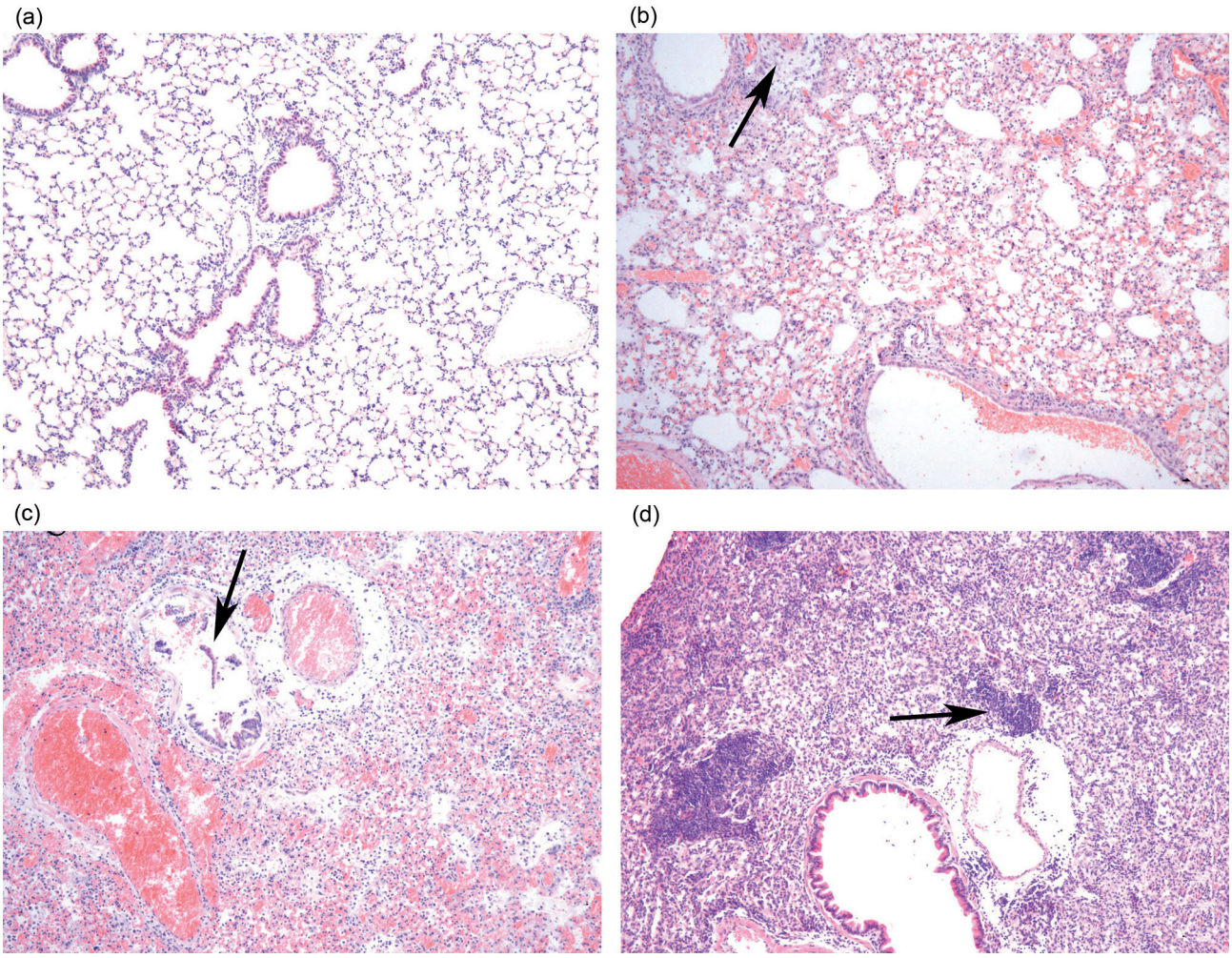

Fig. 2

Effect of SIV infection on lung histopathology of mice

(a) Mock-infection. (b) Mild interstitial edema around small blood vessels and bronchiole and inflammatory cell exudate on day 2 p.i. (c) Moderate bronchioalveolitis with cellular debris in bronchioles and alveoli on day 4 p.i. (d) Severe bronchitis characterized by degeneration and necrosis of bronchial epithelium with intra-luminal cellular debris on day 6 p.i. .Magnification 100x.

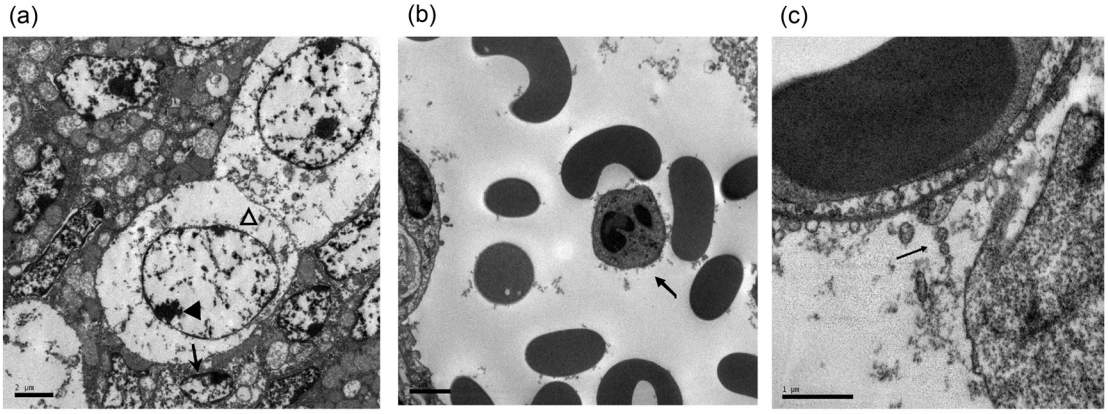

Fig. 3

Effect of SIV infection on the ultrastructure of lung tissue

(a) Pneumocyte edema with nucleolar margination (open triangle), vacuolar degeneration of cytoplasm (solid triangle), mitochondrial edema and vacuolar degeneration (arrow). (b) Hemorrhagic and inflammatory exudates within the alveolar lumen. PMN cells (arrow). (c) Virions in alveolar epithelium (arrow). Magnification bars have been marked with their length in μm.

hemorrhagic necrosis along with PMN cell infiltration was also prominent and seen at different time points (Fig. 3b). Short-stick-shaped and spherical influenza virions could be observed on flat epithelial cell surface of pulmonary alveoli and in alveolar lumen of mice (Fig. 3c).

Lung coefficient and lung W/D ratio

The lung wet weight of H9N2-infected mice increased slightly on day 2 p.i., but there was no statistical significance in the W/D ratio. However, the lung W/D ratio on day 4–6 p.i. increased significantly (P <0.01). On day 8 p.i., W/D ratio of the infected mice began to recover progressively, but it still had significant difference (P <0.01). On day 14 p.i., W/D ratio was close to control data (shown in Fig. 4).

As shown in Fig.5, there was no significant difference of lung coefficient between infected and mock-infected mice on day 2 p.i. However, the lung coefficient of H9N2-infected mice increased dramatically on day 4–8 p.i. (P <0.01). On day 14 p.i., there was no significant difference between H9N2-infected and mock-infected mice (P >0.05) again.

Arterial blood gas characteristics

Table 1 shows the results of blood gas analysis. The partial pressure of arterial oxygen (PaO_2) and oxygen hemoglobin

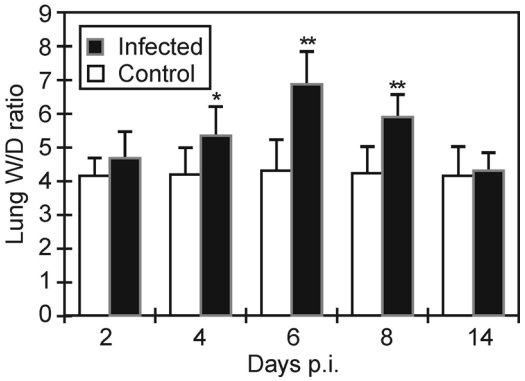

Fig. 4

Effect of SIV infection on the lung D/W ratio in mice

At each time point after H9N2 SIV infection, the infected mice lung wet/dry ratios increased markedly. Data are expressed as mean ± standard error. Open bars = control group; solid bars = inoculated group. *P <0.05 and **P <0.01 compared with control mice.

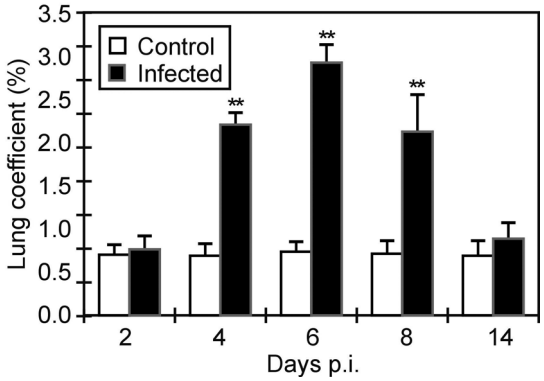

Fig. 5

Effect of SIV infection on the lung coefficient in mice

At each time point after H9N2 SIV infection, the infected mice lung wet weight/body weight increased markedly. Data are expressed as mean ± standard error. Open bars = control group; solid bars = inoculated group. *P <0.05 and **P <0.01 compared with control mice.

Table 1 Effect of SIV infection on arterial blood gas characteristics in mice

Days p.i.		PaO_2 (kPa)	$PaCO_2$ (kPa)	pH	SaO_2 (%)
2	Infected	11.6±1.08	5.56±0.31	7.39±0.035	89.3±1.83
	Control	12.39±1.23	5.28±0.43	7.36±0.071	92.9±1.21
4	Infected	9.38±1.45*	5.98±0.26	7.26±0.079	84.1±2.14*
	Control	12.17±1.46	5.27±0.31	7.34±0.052	93.2±0.95
6	Infected	6.79±1..27**	7.45±0.87	7.23±0.065	78.3±3.78**
	Control	12.51±0.84	5.16±0.82*	7.35±0.027	92.6±1.52
8	Infected	8.85±1.42**	7.39±0.43	7.31±0.086	86.4±2.19**
	Control	12.36±1.28	5.21±0.30*	7.36±0.043	91.9±1.74
14	Infected	11.4±1.31	5.62±0.85	7.35±0.047	90.1±2.34
	Control	12.38±1.74	5.29±0.76	7.37±0.067	93.4±2.82

*/**Significant differences with P <0.05/P <0.01, respectively.

saturation (SaO_2) were slightly decreased, while the partial pressure of arterial carbon dioxide ($PaCO_2$) increased (P <0.05) and pH value decreased in H9N2-infected mice on day 2 p.i. However, pH value, PaO_2 and SaO_2 of the most infected mice decreased (P <0.01), and $PaCO_2$ increased significantly on day 4–6 p.i. On day 8 p.i., the results were similar to those of day 6 p.i. Decrease of PaO_2 was only 1/2 of that of control mice, while $PaCO_2$ increased dramatically (Table 2).

BALF inflammatory cells

The total number of inflammatory cells in BALF of H9N2-infected mice increased from day 2 p.i., and the increase became obvious on day 4–8 p.i. (P <0.01). From day 2 p.i., the ratio of lymphocytes and especially PMNs (P <0.01) in BALF started to increase. By contrast, there was a slight decrease in ratio of alveolar macrophages, which reached the highest level on day 6 p.i. with significant difference in comparison with control mice. From 8 day p.i., the number of PMNs and lymphocytes started to decrease, however, the significant difference compared with controls was still visible.

Discussion

Pigs, acting as an intermediate host for avian and human influenza virus, can play a very important role in the epidemic of human influenza. H9N2 SIV is one of the major epidemic subtypes which have caused swine influenza so far, and the recombinant virus containing human-avian-swine influenza viruses has already been described (Sullivan *et al.*, 2010). If the strain acquires the ability to bind human cell surface receptors, there might be a threat of H9N2 swine influenza epidemic.

In this study, BALB/c mice inoculated with A/swine/HeBei/012/2008/ (H9N2) virus displayed inactivity, inappetence and weight loss. From days 3 to 8 p.i., respiratory frequency increased and respiratory distress occurred and resulted in 62.5% mortality. Hemorrhage, severe edema and

Table 2 Effect of SIV infection on total and differential leukocyte counts in mice

Days p.i.		Total leukocyte count (1×10^8/ml)	Differential leukocyte count (%)		
			Macrophages	Lymphocytes	PMNs
2	Infected	2.89±0.37*	46.26±4.73*	45.12±3.75*	2.96±1.43**
	Control	1.47±0.36	65.9±8.51	32.37±6.69	0.98±0.63
4	Infected	4.18±0.32**	37.7±6.37**	56.39±4.27**	6.04±2.31**
	Control	1.89±0.61	73.74±4.69	21.64±5.12	2.87±0.33
6	Infected	12.69±2.13**	25.12±3.54**	47.37±3.76**	21.64±4.47**
	Control	1.74±0.41	82.23±2.47	18.32±5.54	1.42±0.39
8	Infected	9.38±3.95**	28.25±1.62**	42.42±4.73**	18.43±6.27**
	Control	1.48±0.62	87.52±3.65	10.75±3.19	0.92±0.34
14	Infected	2.21±0.84	64.34±4.28	36.53±3.32	2.15±0.38
	Control	1.38±0.25	88.78±1.62	9.21±1.75	0.91±0.42

*/**Significant differences with P <0.05/P <0.01, respectively.

plenty of blood-red frothy exudate was found in the lungs of infected mice. Meanwhile, the lung coefficient and lung W/D ratio increased significantly, as a sign of severe lung edema. Histopathological observation confirmed that H9N2 SIV infection caused viral interstitial pneumonia characterized by diffuse and exudative inflammation with obvious alveolar and interstitial edema, significant inflammatory cell exudate in alveolar lumen and interstitium. Plenty of inflammatory cells, erythrocytes, and epithelial debris around bronchus and inside lumen were found as well. The results of this study were consistent with the histopathological features of ALI/ARDS. Meanwhile, these changes are consistent with the histopathological lesions of ALI/ARDS, which were induced by inoculation of CBA/J mice with reovirus 1/L strains by London and his co-workers (London *et al.*, 2002). Others have found that after infection, follicular bronchitis and lymphatic folliculitis around vessels developed from original bronchiole flake pneumonia (Fagan *et al.,* 1999). Furthermore, our findings are also consistent with the pathological findings from studies on H9N2 avian influenza virus impact on mice by Deng and colleagues (Deng *et al.,* 2010). In these studies, the infected mice displayed a similar histopathologic pattern, including peribronchiolar patchy pneumonia – bronchiolitis - bronchopneumonia. Hence, the pathological changes in H9N2 SIV infected mice were consistent with that of ALI, that is, the inflammatory cellular infiltration, interstitial and alveolar edema, and hemorrhage were observed in the lungs.

Both, the number of ventilated alveoli and thickness between alveoli-capillary membranes can influence exchange of oxygen in alveoli and erythrocytes in blood. Studies have demonstrated that virus infections lead to impairment of the alveolar epithelium and vascular endothelium, which increases the thickness of alveolar-capillary membranes and influences the function of oxygen exchange, resulting in hypoxia (Headley *et al.*, 1997). Arterial blood gas exchanges were studied to confirm whether the serious histopathological injury of lungs caused by A/swine/HeBei/012/2008 (H9N2) virus infection leads to hypoxemia during the infection process. The results indicated that PaO_2 and SaO_2 of the infected mice decreased significantly, while $PaCO_2$ increased, indicating the presence of severe hypoxemia in mice (PaO_2 was 6.79 kPa ± 1.27 kPa, lower than 8 kPa, $PaCO_2$ was 7.45 kPa ± 0.87 kPa, higher than 6.67 kPa). During hypoxemia phase of the illness, the corresponding histopathological changes of the mice lungs showed diffuse alveolar injury and dysfunction of ventilation function between pulmonary alveoli and capillary, which resulted in hypoxemia. Clinical symptoms comprised of increase in respiratory rate, occurrence of respiratory distress, and lung failure. Our results showed that serious progressive hypoxemia occurred in mice during the process of A/swine/HeBei/012/2008/ (H9N2) virus infection.

In this study, after intranasal inoculation of A/swine/HeBei /012/2008/ (H9N2) influenza virus, the mice showed acute onset of the disease, urgent breathing and expiratory dyspnea. Diffuse alveolar injury was the main feature of histopathological changes. Progressive hypoxemia resulted from biased ventilation function. All above mentioned symptoms corresponded with clinical characteristics and pathophysiological changes of ALI/ARDS.

In this report, we described a mouse model of ALI induced by H9N2 SIV, which demonstrated that BALB/c mice become ill when inoculated intranasally with H9N2 virus. Furthermore, studies on cynomolgus macaques infected with new type of H1N1 virus by Herfst *et al.* also showed that the virus could cause pathological changes in lungs with diffuse alveolar injury as its main feature (Herfst *et al.,* 2010), and the changes were similar with that of development process of H9N2 SIV infection in mice. Therefore, the investigations on mice models infected with H9N2 SIV in this study not only makes it possible to provide a basis for the prevention and treatment of H9N2 infections, but also helps to explore the treatment for human ALI induced by new H1N1 virus.

Acknowledgement. This work was supported by the grant No. C2009001028 and C2011405002 from the Natural Science Foundation of HeBei province of China. The authors thank Dr. Vivek K. Rauniyar of Hebei North University for providing his valuable suggestions and help in the preparation of this manuscript.

References

Bernard GR (2005): Acute respiratory distress syndrome: a historical perspective. Am. J. Respir. Crit. Care. Med. 172, 798–806. http://dx.doi.org/10.1164/rccm.200504-663OE

Bernard GR, Artigas A, Brigham KL, Carlet J, Falke K, Hudson L, Lamy M, Legall JR, Morris A, Spragg R (1994): The American-european consensus conference on ARDS: definitions, mechanisms, relevant outcomes, and clinical trial coordination. Am. J. Respir. Crit. Care. Med. 149, 818–824.

Butt KM, Smith GJ, Chen H, Zhang LJ, Leung YH, Xu KM, Lim W, Webster RG, Yuen KY, Peiris JS, Guan Y (2005): Human infection with an avian H9N2 influenza A virus in Hong Kong in 2003. J. Clin. Microbiol. 43, 5760–5767. http://dx.doi.org/10.1128/JCM.43.11.5760-5767.2005

Cong YL, Pu J, Liu QF, Wang S, Zhang GZ, Zhang XL, Fan WX, Brown EG, Liu JH (2007): Antigenic and genetic characterization of H9N2 swine influenza viruses in china. J. Gen. Virol. 88, 2035–2041. http://dx.doi.org/10.1099/vir.0.82783-0

Cong YL, Wang CF, Yan CM, Peng JS, Jiang ZL, Liu JH (2008): Swine infection with H9N2 influenza viruses in China in 2004. Virus Genes 36, 461–469. http://dx.doi.org/10.1007/s11262-008-0227-z

Deng G, Bi J, Kong F, Li X, Xu Q, Dong J, Zhang M, Zhao L, Luan Z, Lv N, Qiao J (2010): Acute respiratory distress syndrome induced by H9N2 virus in mice. Arch. Virol. 155, 187–195. http://dx.doi.org/10.1007/s00705-009-0560-0

Fagan KA, Fouty BW, Tyler RC, Morris KG Jr, Hepler LK, Sato K, LeCras TD, Abman SH, Weinberger HD, Huang PL, McMurtry IF, Rodman DM (1999): The pulmonary circulation of homozygous or heterozygous eNOS-null mice is hyperresponsive to mild hypoxia. J. Clin. Invest. 103, 291–299. http://dx.doi.org/10.1172/JCI3862

Fagan KA, Oka M, Bauer NR, Gebb SA, Ivy DD, Morris KG, McMurtry IF (2004): Attenuation of acute hypoxic pulmonary vasoconstriction and hypoxic pulmonary hypertension in mice by inhibition of Rho-kinase. Am. J. Physiol. Lung Cell Mol. Physiol. 287, 656–664. http://dx.doi.org/10.1152/ajplung.00090.2003

Hudson LD, Steinberg KP (1999): Epidemiology of acute lung injury and ARDS. Chest 116, 74–82. http://dx.doi.org/10.1378/chest.116.suppl_1.74S-a

Herfst S, van den Brand JM, Schrauwen EJ, de Wit E, Munster VJ, van Amerongen G, Linster M, Zaaraoui F, van Ijcken WF, Rimmelzwaan GF, Osterhaus AD, Fouchier RA, Andeweg AC, Kuiken T (2010): Pandemic 2009 H1N1 influenza virus causes diffuse alveolar damage in cynomolgus macaques. Vet. Pathol. 47, 1040–1047. http://dx.doi.org/10.1177/0300985810374836

Headley AS, Tolleye, Meduel GU (1997): Infection and inflammatory response in acute respiratory distress syndrome. Chest 111, 1306–1321. http://dx.doi.org/10.1378/chest.111.5.1306

Lin YP, Shaw M, Gregory V, Cameron K, Lim W, Klimov A, Subbarao K, Guan Y, Krauss S, Shortridge K, Webster R, Cox N, Hay A (2000): Avian-to-human transmission of H9N2 subtype influenza Aviruses: Relationship between H9N2 and H5N1 human isolates. Proc. Natl. Acad. Sci. USA 97, 9654–9658. http://dx.doi.org/10.1073/pnas.160270697

London L, Majeski E I, Paintlia M K, Harley H A, London S D (2002): Respiratory reovirus 1/L induction of diffuse alveolar damage: A model of acute respiratory distress syndrome. J. Exp. Mol. Pathol. 103, 24–36. http://dx.doi.org/10.1006/exmp.2001.2414

Majeski EI, Paintlia MK, Lopez AD, Harley RA, London SD, London L (2003): Respiratory reovirus 1/L induction of intraluminal fibrosis, a model of bronchiolitis oblitreans organizing pneumonia, is dependent on T lymphocytes. Am. J. Pathol. 163, 1467–1479. http://dx.doi.org/10.1016/S0002-9440(10)63504-3

Peiris JS, Guan Y, Markwell D, Ghose P, Webster RG, Shortridge KF (2001): Co-circulation of avian H9N2 and contemporary "human"H9N2 influenza A viruses in pigs in southeastern China: Potential for genetic reassortment? J. Virol. 75, 9679–9686. http://dx.doi.org/10.1128/JVI.75.20.9679-9686.2001

Sullivan SJ, Jacobson RM, Dowdle WR, and Poland GA (2010): 2009 H1N1 Influenza. Mayo Clin. Proc. 85, 64–76. http://dx.doi.org/10.4065/mcp.2009.0588

Wan H, Perez DR (2007): Amino acid 226 in the hemagglutinin of H9N2 influenza viruses determines cell tropism and replication in human airway epithelial cells. J. Virol. 81, 5181–5191. http://dx.doi.org/10.1128/JVI.02827-06

Xu T, Qiao J, Zhao LH, Wang GR, He GM, Li K, Tian Y, Gao MY, Wang JL, Wang HY, Dong CG (2006): Acute respiratory distress syndrome induced by Avian influenza A (H5N1) virus in mice. Am. J. Respir. Crit. Care Med. 174, 1011–1017. http://dx.doi.org/10.1164/rccm.200511-1751OC

Yu H, Hua RH, Wei TC, Zhou YJ, Tian ZJ, Li GX, Liu TQ, Tong GZ (2008): Isolation and genetic characterization of avian origin H9N2 influenza viruses from pigs in China. Vet. Microbiol. 131, 82–92. http://dx.doi.org/10.1016/j.vetmic.2008.02.024